SCIENCE CHINA
Technological Sciences

January 2013 Vol.56 No.1: 137–142
doi: 10.1007/s11431-012-5042-z

Theoretical study on boiling heat transfer in the Xi'an pulsed reactor

CHEN LiXin[1,2*], TANG XiaoBin[1], JIANG XinBiao[2], CHEN Da[1] & ZHAO ZhuMin[2]

[1] *Department of Nuclear Science & Engineering, Nanjing University of Aeronautics & Astronautics, Nanjing 210016, China;*
[2] *Northwest Institute of Nuclear Technology, Xi'an 710024, China*

Received July 24, 2012; accepted September 3, 2012; published online October 10, 2012

Boiling heat transfer condition has significance for pool-type research reactors cooled by natural circulation. It has important effect on the fuel element safety of reactor. On the basis of heat transfer characteristics of the Xi'an pulsed reactor (XAPR), fuel conduction, single-phase convection and boiling heat transfer, and void fraction models of the core are constructed. To validate the correctness of the physical models presented in the paper, numerical calculation based on a subchannel analysis method of XAPR is carried out, and the temperature fields are measured in some reactor coolant channels. The comparison between the calculated and experimental results verifies the effectiveness of the models. These physical models are used to calculate the thermal-hydraulic parameters of XAPR at the rated power (for XAPR the rated power is 2.0 MW in steady-state operation). The results indicate that subcooled boiling occurs in the XAPR core but it exhibits a subcooling degree which is considerably higher than that of saturation boiling. Subcooled boiling improves the efficiency of heat transfer between the fuel element surface and coolant, as well as effectively protects fuel elements. This research is also a beneficial reference in thermal-hydraulic analysis for other natural circulation reactors.

pulsed reactor, thermal-hydraulic analysis, subcooled boiling, heat transfer coefficient, void fraction

Citation: Chen L X, Tang X B, Jiang X B, et al. Theoretical study on boiling heat transfer in the Xi'an pulsed reactor. Sci China Tech Sci, 2013, 56: 137–142, doi: 10.1007/s11431-012-5042-z

1 Introduction

Subcooled boiling may occur when the liquid flows into a heated section that has a high heat flux and/or wall temperature. It is a well-known heat transfer modality between solid and liquid phases. In the past several decades, subcooled boiling has attracted considerable research attention because of its high heat transfer efficiency [1–3]. For some natural circulation pool-type reactors, subcooled boiling in the reactor core is an accepted practice and facilitates the fuel element cooling. However, high element clad-coolant heat flux that is close to critical heat flux (CHF) point presents hazards to the fuel element clad. Thus, the heat transfer characteristics of subcooled boiling are important in the reactor thermal-hydraulic design.

The Xi'an pulsed reactor (XAPR), a pool-type research reactor cooled by natural circulation of water, is installed at the Northwest Institute of Nuclear Technology of China. XAPR employs a cylindrical fuel-moderator element, in which the zirconium-hydride moderator is homogeneously combined with 19.7% enriched uranium. XAPR has two types of core arrangements: steady-state and pulsed modes. It has a rated power of 2000 kW under steady-state operation and a pulsed peak power of 4300000 kW at pulsed operation. The core of the XAPR has a working pressure as low as 0.17 MPa and a maximal fuel temperature of approximately 780 K at the rated operating conditions.

*Corresponding author (email: chelson@126.com)

In the XAPR design stage, heat transfer between the fuel element clad and the coolant is considered of single-phase natural circulation. The heat transfer characteristics of sub-cooled boiling are disregarded in the initial thermal-hydraulic analysis because of the low thermal power of the reactor. Under high-power operation of XAPR, bubbles are observed in the central cave of the core. Bubbles move with coolant and cannot be condensed locally, indicating that boiling heat transfer occurs in the reactor core. This boiling phenomenon means that the clad temperature has reached the saturation temperature of the coolant under working pressure. The flow field becomes turbulent by the bubbles that form on the surface of the fuel element, and the bubbles improve the heat transfer coefficient of natural circulation. If the wall temperature of the fuel element continually increases, the increased bubbles will cover the fuel element surface. Vapor therefore forms an insulating blanket that covers the clad and increases the clad surface temperature rapidly. This heat transfer conduction is called film boiling. By further increasing the wall temperature, the heat transfer rate is also increased by thermal radiation. However, too high a temperature would damage the fuel element clad. This study aims to identify the subcooled boiling heat transfer condition between the fuel element and the coolant in the XAPR core, as well as analyze the safety effects of bubbles.

2 Physical model

2.1 Fuel element heat conduction

The XAPR rod is cylindrical, with an outer diameter of 37.2 mm, a total length of 760 mm, and a mass of 3.32 kg. The rod is composed of a stainless steel clad, $UZrH_{1.6}$ fuel, and zirconium mandril. The gap with helium gas between the fuel and the clad is designed to control fuel swelling and improve heat transfer conditions. Figure 1 shows the geometry of the XAPR fuel element.

For the fuel element of XAPR, one-dimensional heat conduction equation may be written as

$$\rho c\frac{\partial T}{\partial t}=\frac{1}{f(x)}\frac{\partial}{\partial x}\left[kf(x)\frac{\partial T}{\partial x}\right]+S, \tag{1}$$

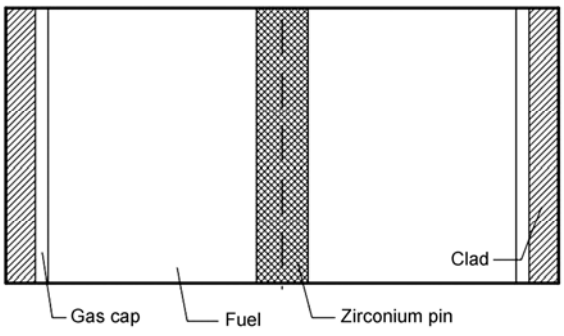

Figure 1 Geometry of the XAPR fuel element.

where x is the direction of heat conduction, $f(x)$ is a function that is connected to the heat conduction area, S is the heat source, k denotes the heat conduction coefficient, and T represents the temperature.

Based on the structure of the XAPR fuel element, heat conduction equation (1) is rewritten as the following four equations:

(1) Zr-mandril heat conduction equation:

$$\rho_{\mathrm{Zr}}c_{\mathrm{Zr}}\frac{\mathrm{d}T_{\mathrm{Zr}}}{\mathrm{d}t}=\frac{1}{r}\frac{\mathrm{d}}{\mathrm{d}r}\left[k_{\mathrm{Zr}}r\frac{\mathrm{d}T_{\mathrm{Zr}}}{\mathrm{d}r}\right]. \tag{2}$$

(2) Fuel heat conduction equation:

$$\rho_{\mathrm{fuel}}c_{\mathrm{fuel}}\frac{\mathrm{d}T_{\mathrm{fuel}}}{\mathrm{d}t}=\frac{1}{r}\frac{\mathrm{d}}{\mathrm{d}r}\left[k_{\mathrm{fuel}}r\frac{\mathrm{d}T_{\mathrm{fuel}}}{\mathrm{d}r}\right]+q_v. \tag{3}$$

(3) Gas-cap heat conduction equation:

$$\rho_{\mathrm{gas\text{-}gap}}c_{\mathrm{gas\text{-}gap}}\frac{\mathrm{d}T_{\mathrm{gas\text{-}gap}}}{\mathrm{d}t}=\frac{1}{r}\frac{\mathrm{d}}{\mathrm{d}r}\left[k_{\mathrm{gas\text{-}gap}}r\frac{\mathrm{d}T_{\mathrm{gas\text{-}gap}}}{\mathrm{d}r}\right]. \tag{4}$$

(4) Clad heat conduction equation:

$$\rho_{\mathrm{clad}}c_{\mathrm{clad}}\frac{\mathrm{d}T_{\mathrm{clad}}}{\mathrm{d}t}=\frac{1}{r}\frac{\mathrm{d}}{\mathrm{d}r}\left[k_{\mathrm{clad}}r\frac{\mathrm{d}T_{\mathrm{clad}}}{\mathrm{d}r}\right]. \tag{5}$$

In the four equations, ρ denotes the material density, kg m^{-3}; c is the specific heat, J $(kg\ K)^{-1}$; k represents the heat conduction coefficient, W $(mK)^{-1}$; T is the temperature, K; q_v is the volume power density, W m^{-3}.

2.2 Heat transfer between clad and coolant

The heat transfer between clad surface and coolant is a natural convection heat transfer, which can be separated into four different regimes, namely, single-phase convection regime, nucleate boiling regime, transition boiling (or partial film boiling) regime, and stable film regime. In this work, a suitable heat transfer correlation for each regime is derived.

In laminar tube flow (single phase flow), the heat transfer efficiency is calculated by the Sieder-Tate correlation [4]:

$$Nu=1.86(Re\ Pr)^{1/3}\left(\frac{d}{L}\right)^{1/3}\left(\frac{\mu_{\mathrm{flow}}}{\mu_{\mathrm{wall}}}\right)^{0.14}$$

$$\text{for } (RePr)d/L\geqslant 10, \tag{6}$$

where μ is the dynamic viscosity (pa s), which is evaluated at the wall temperature; Re is Reynolds number; Pr is Prandtl number; and Re, Pr, and μ_{flow} are evaluated under the average coolant temperature.

For the subcooled nucleate boiling regime, the wall superheat is determined using the correlation proposed by

McAdams [5]:

$$q_{\text{nucl}} = 2.257 \times (T_{\text{wall}} - T_{\text{sat}})^{3.86}. \quad (7)$$

The equivalent heat transfer efficiency is

$$h_{\text{nucl}} = q_{\text{nucl}} / (T_{\text{wall}} - T_{\text{flow}}), \quad (8)$$

where q_{nucl} is the heat flux in the subcooled nucleate boiling regime, W cm^{-2}; h_{nucl} is equivalent heat transfer coefficient, W (cm^{-2} K^{-1}); T_{flow} is the average coolant temperature, K; T_{sat} is the coolant saturation temperature, K. When the system pressure approaches 0.1 MPa, the nucleate boiling regime is narrow, and the wall temperature is limited to T_{sat}+ 5 K$\leqslant T_{\text{wall}} \leqslant T_{\text{sat}}$+25 K in eq. (7).

Boiling becomes unstable in the transition boiling regime. The heat surface is alternately covered with a vapor blanket and a liquid layer, resulting in oscillating surface temperature. In engineering calculation, a boiling curve in the logarithmic coordinate system is typically used at this regime. For this method, the heat transfer coefficient can be calculated by linear interpolation between the critical heat flux q_{CHF} and the minimum heat flux q_{min}. Eq. (9) shows this correlation [6]:

$$\ln \frac{q_{\text{CHF}}}{q_{\text{local}}} = \frac{(\ln q_{\text{CHF}} - \ln q_{\text{min}})(\ln \Delta T_{\text{wall}} - \ln \Delta T_{\text{CHF}})}{\ln \Delta T_{\text{min}} - \ln \Delta T_{\text{CHF}}}. \quad (9)$$

where q_{local} is the local heat flux, W cm^{-2}; q_{CHF} is the critical heat flux, W cm^{-2}; q_{min} denotes the minimum heat flux in the transition boiling regime, W cm^{-2}; T_{min} refers to minimum temperature, K.

Because the mechanism of film boiling is difficult to recognize, no theory currently explains this regime. The existing calculation methods depend on simulations of experimental results, which present narrow applicability. Film boiling is an interdicted heat transfer condition in the pulsed reactor engineering design; thus, it is not the focus of this research. The heat transfer coefficient of film boiling is calculated with eqs. (10) and (11), in accordance with engineering practice [7]. In accordance with different wall temperatures, the heat transfer condition is separated into two stages, expressed as

$$q_{\text{film}} = 5.945 \times 10^2 \times \Delta T_{\text{sat}}^{0.747}, \quad (10)$$

$$q_{\text{film}} = 2.439 \times 10^{-2} \times \Delta T_{\text{sat}}^{2.308}, \quad (11)$$

where q_{film} is the heat flux produced by single-phase turbulent flow, W cm^{-2}. The separation point of the two stages is decided by the point of intersection of eqs. (10) and (11).

2.3 Two-phase flow model

For the vapor-liquid, two-phase flow of the coolant channel in XAPR, the Euler multiphase flow equation can be used:

$$\frac{\partial}{\partial \tau}(\beta_i \rho_i \phi_i) + \nabla \cdot (\beta_i \rho_i U_i \phi_i) = \nabla \cdot \left(\beta_i \alpha_i \nabla \phi_i\right) + S_i + C_{12}(\phi_2 - \phi_1), \quad (12)$$

where β_i is the volume fraction of phase i (i = 1, 2 refers to a different phase), ρ_i is the density of phase i, kg m^{-3}; φ_i refers to different general parameters in different conservation equations; U_i is the velocity vector of phase i, m s^{-1}; α_i refers to viscosity of phase i in the momentum conservation equation; α_i is the heat transfer efficiency of phase i for the energy conservation equation, S_i denotes the source item; $C_{12}(\varphi_2 - \varphi_1)$ refers to transfer item between phases 1 and 2 of φ_i. The mass, momentum, and energy conservation equations can be written according to eq. (12). These equations are discussed in ref. [8].

Using microlayer evaporation theory as basis, Judd and Hwang [9] indicate that the heat flux of subcooled boiling can be divided into three components, expressed as follows:

$$q_{\text{wall}} = q_{\text{sing-phase}} + q_q + q_e, \quad (13)$$

where q_{wall} is the wall heat flux of subcooled boiling regime, q_{sp} is the heat flux of the coolant in single-phase heat transfer, q_{ev} is the heat flux produced by the coolant evaporation in the microlayer, and q_{bubble} is the heat flux produced by the sensible heat of fluid that occupies the volume evacuated by a departing bubble. The heat transfer area quotient of the wall for single-phase convection is denoted as A_1 and the other two parts of the heat transfer area quotient are denoted as A_2. Thus, $A_1 + A_2 = 1$.

$$q_{\text{sp}} = h_{\text{sp}} A_1 (T_{\text{wall}} - T_{\text{flow}}), \quad (14)$$

$$q_{\text{ev}} = \left[\frac{2}{\sqrt{\pi}} f \sqrt{\tau k_{\text{flow}} \rho_{\text{flow}} c_{\text{pf}}} \right] A_2 (T_{\text{wall}} - T_{\text{flow}}), \quad (15)$$

$$q_{\text{bubble}} = \dot{m} h_{\text{bubble}}, \quad (16)$$

where h_{sp} is the overall heat transfer coefficient of single-phase convection, $h_{\text{sp}} = St \cdot \rho_{\text{f}} \cdot C_{\text{pf}} \cdot u_{\text{f}}$; St is the local Stanton number, $St = Nu/(RePr)$; f denotes the bubble departure frequency, s^{-1}; c_{pf} represents the specific heat at constant pressure, J kg^{-1} K^{-1}; τ is the bubble waiting period, s. Bubble departure period f^{-1} equals the sum of the growth and waitting periods. Kurul assumed that the bubble waiting period is 80% of the departure period, and $\tau = 0.8 \cdot f^{-1}$; $\dot{m}$ is the bubble departure mass rate per unit area of the heat surface; h_{bubble} refers to the latent heat of the bubble, J kg^{-1} [10].

Bubble departure diameter is calculated by Unal's model, which is based on microlayer evaporation and energy balance theory [11]. Bubble average diameter is calculated by Zeitoum's model [12], and bubble departure frequency is calculated by Cole's correlation [13].

3 Experiment and validation of the model

To determine the distribution of the temperature field of the XAPR core, an experiment that measures the temperature values in typical channels is conducted. For the experiment, several thermocouples are arranged in the typical channels of the core. For XAPR, a fuel temperature measurement element is arranged at the C10 cell. Figure 2 shows the arrangement of the measurement point of thermocouples in the core. Figure 3 shows the structure of the fuel temperature measurement element and its position in the core. The values of the temperature measurement element are also recorded.

To validate the model of the natural circulation heat transfer of XAPR, several thermal-hydraulic parameters of the core in different power stages are analyzed with the single-channel method. Figure 4 shows the coolant channel section of XAPR; the shadowed area indicates the coolant channel section. After calculation, the calculation results and experimental measurements are compared (Table 1). The comparison indicates that the calculation and experimental results are in good agreement.

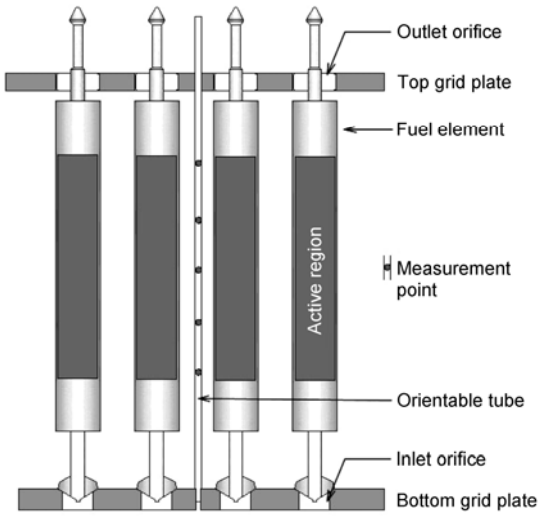

Figure 2 Measurement points of thermocouples in the core.

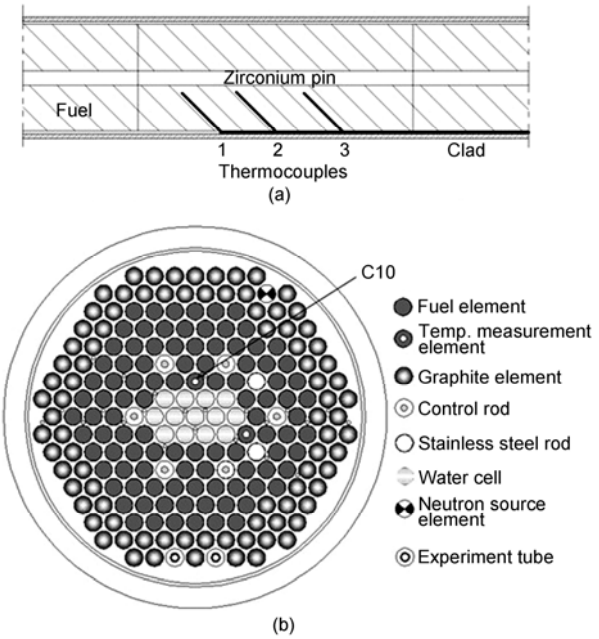

Figure 3 Structure of the temperature measurement element and its position in the core. (a) Structure of the temperature measurement element; (b) temperature measurement position in the core.

4 Results and discussion

The steady-state analyses of XAPR are presented in this section. The thermal-hydraulic parameters at rated operating conditions (2.0 MW) are calculated and listed in Table 2. In the calculation, the distribution of coolant mass flow is assumed to be an average value.

To elucidate the temperature field and the bubble distribution in the XAPR core, the temperature variations of the hottest fuel element are plotted in Figure 5.

Figure 5 shows that the temperature curve of the fuel is distributed in the axial direction as a cosine function, and

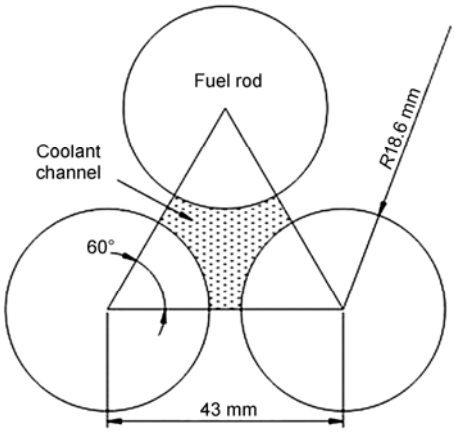

Figure 4 Subchannel sketch of XAPR.

Table 1 Comparison of experimental and calculated results

Power (MW)	Fuel temperature (K)		Coolant temperature (K)		
			Channel 1	Channel 2	Channel 3
1.0	Measured	591	296	296	304
	calculation	586.1	295.3	295.3	303.4
	error (%)	0.83	0.24	0.24	0.20
1.5	Measured	694	300	302	315
	calculation	678.9	300.0	300.2	312.2
	error (%)	2.18	0.00	0.60	0.89
2.0	Measured	772	301	306	320
	calculation	765.6	304.0	303.9	320.1
	error (%)	0.83	–1.00	0.69	–0.03

Table 2 Thermal-hydraulic parameters of XAPR at 2.0 MW

Parameter	Value
Thermal power (MW)	2.0
System pressure (MPa)	0.17
Core inlet temperature (K)	308.2
Coolant mass flux (kg s^{-1})	12.13
Rod average heat flux (MW m^{-2})	0.414
Rod maximal heat flux (MW m^{-2})	0.708
MDNBR	2.36
Fuel central maximal temperature (K)	777.0
Fuel edge maximal temperature (K)	422.6
Clad maximal temperature (K)	405.8
Average channel	
Outlet temperature (K)	320.3
Outlet void fraction (%)	0.84
Average bubble diameter (mm)	1.58
Bubble diameter zone (mm)	1.5–2.5
Hot channel	
Outlet temperature (K)	363.0
Outlet void fraction (%)	3.31
Average bubble diameter (mm)	2.35
Bubble diameter zone (mm)	1.7–3.4

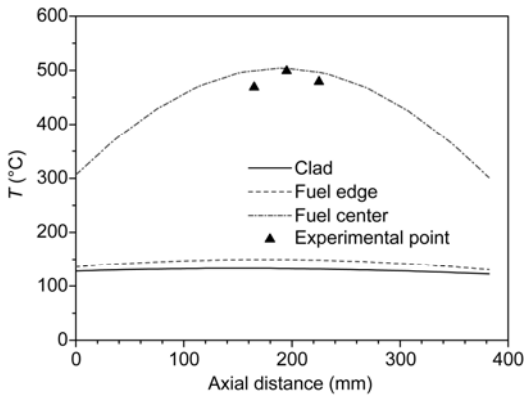

Figure 5 Axial temperature distribution of the rod at rated power conditions.

that the maximal temperature value lies in the center of the fuel axial direction. The clad temperature slightly changes along the axial direction because of the excellent heat conduction performance of stainless steel.

Figure 6 shows the temperature variations of the hot channel and the average channel of the core at rated operating conditions. The outlet temperature difference between the hot and average channels is about 40 K.

After the analysis of the rated power, some thermal parameters are calculated for different power stages; that is, 500, 1000, and 1500 kW. The axial void fraction curves of the hot channel in different power stages are shown in Figure 7. Subcooled boiling occurs in the hot channel when the reactor power is approximately 500 kW, but the bubbles are condensed by the coolant before arrival at the channel outlet. With increasing power, the subcooling degree continuously decreases. Thus, the bubbles are condensed but gradually

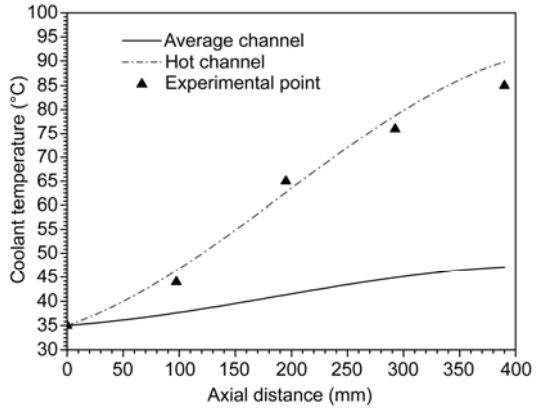

Figure 6 Axial temperature distribution in the coolant channel at rated power conditions.

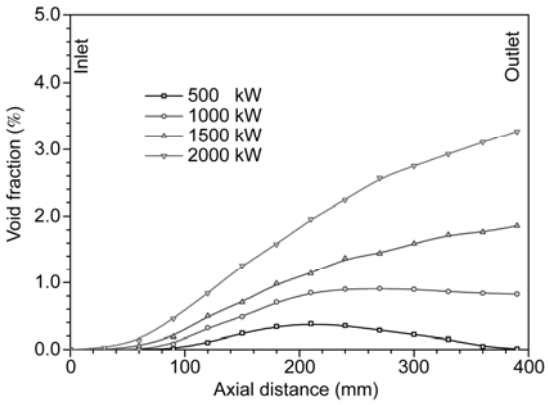

Figure 7 Coolant void fraction of the hot channel at different power stages.

collected in the channel.

The results for the void fraction and the numerical simulation of bubble diameter at the rated power conditions are shown in Figures 8 and 9.

The maximum surface temperature of the fuel element is higher than the coolant saturation temperature under the same pressure, indicating that subcooled boiling condition occurs in several channels of XAPR. The bubbles have a low diameter but cannot be condensed in the core. Numerous bubbles accumulate in the chimney down to the top grid plate of the channel, and gradually expand. The bubbles overflow through the outlet orifices in the top grid plate. Finally, the bubbles are condensed by water in the reactor pool.

5 Conclusions

Thermal-hydraulic calculation models are developed on the basis of the heat transfer characteristic of XAPR. In these models, the heat conduction in the fuel element, the subcooled boiling between the clad and the coolant, and the

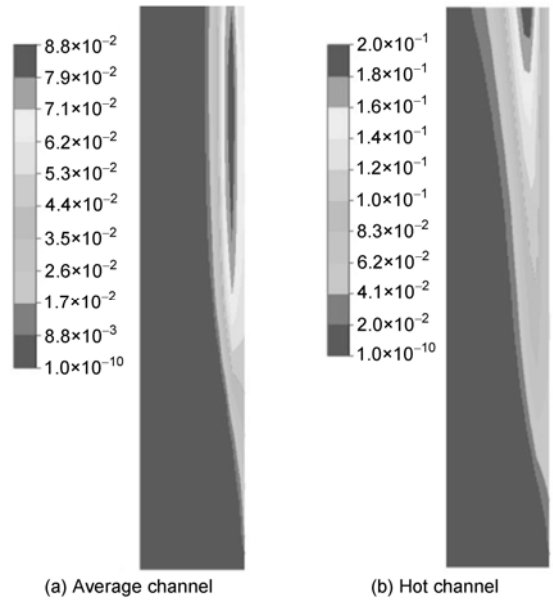

Figure 8 Void fraction distributions in coolant channels.

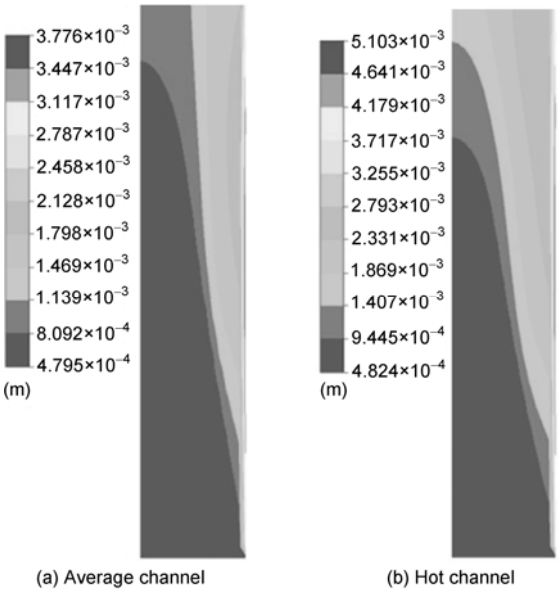

Figure 9 Average bubble diameter distribution in coolant channels.

void fraction of the coolant are comprehensively considered. Single-channel numerical analysis is performed to calculate the thermal-hydraulic parameters of the core. The comparison of the experimental and calculated values indicates that the calculation results are accurate. The comparison also validates the effectiveness of the models constructed in this paper.

The conclusions derived are summarized as follows:

(1) Subcooled boiling occurs in the XAPR core at high power, but the degree of subcooling is considerably higher than that of saturation boiling.

(2) Bubbles in the coolant increase with rising reactor power.

(3) Bubbles formation in the coolant channels accelerates fluid flow velocity and effectively disturbs the flow field, thereby improving heat transfer conditions.

1 Yang J, Guo L J, Zhang X M. A numerical simulation of pool boiling using CAS model. Int J Heat Mass Tran, 2003, 46: 4789–4797
2 Sateesh G, Das S K, Balakrishnan A R. Analysis of pool boiling heat transfer effect of bubbles sliding on the heating surface. Int J Heat Mass Tran, 2005, 48: 1543–1553
3 Xiao B Q, Yu B M. A fractal analysis of subcooled flow boiling heat transfer. Int J Multiphas Flow, 2007, 33: 1126–1139
4 Holman J P. Heat Transfer. New York: McGraw-Hill, 2002
5 Tong L S, Weisman J. Thermal Analysis of Pressurized Water Reactors. 3rd ed. La Grange, Illinois: American Nuclear Society, 1996
6 Xu J. Boiling Heat Transfer and Gas-Liquid Two-phase Flow (in Chinese). Beijing: Atomic Energy Press, 2001
7 Jing C Y. Studies on kinetic characteristics and loss-of-coolant accident for pulsed reactor (in Chinese). Doctoral Dissertation. Xi'an: Xi'an Jiaotong University, 1999
8 Tao W Q. Numerical Heat Transfer (in Chinese). 2nd ed. Xi'an: Xi'an Jiaotong University Press, 2001
9 Judd R L, Hwang R L. A comprehensive model for nucleate pool boiling heat transfer including micro-layer evaporation. ASME J Heat Transf, 1976, 98: 623–629
10 Kurul N, Podowski M Z. Multidimensional effects in sub-cooled boiling. The 9th Heat Transfer Conference. Jerusalem, Israel, 1990
11 Unal H C. Maximum bubble diameter, maximum bubble growth time and bubble growth rate. Heat Mass Transfer, 1976, 19: 643–649
12 Zeitoun O, Shoukri M. Bubble behavior and mean diameter in sub-cooled flow boiling. Heat Transfer, 1996, 118(1): 110–116
13 Cole R. A photographic study of pool boiling in the region of the critical heat flux. AIChE J, 1960, 6: 533–542